PERGAMON

International Journal of Solids and Structures 40 (2003) 5287–5303

INTERNATIONAL JOURNAL OF SOLIDS and STRUCTURES

www.elsevier.com/locate/ijsolstr

The effective electroelastic property of piezoelectric media with parallel dielectric cracks

X.D. Wang *, L.Y. Jiang

Department of Mechanical Engineering, 4-9 Mechanical Engineering Building, University of Alberta, Edmonton, Alberta, Canada T6G 2G8

Received 22 November 2002; received in revised form 17 April 2003

Abstract

Existing studies on the coupled electroelastic behaviour of cracked piezoelectric media have been based mostly on the electrically impermeable and permeable crack models. The current paper presents a study of the effective electroelastic property of piezoelectric media weakened by parallel cracks using a dielectric crack model with the electric boundary condition along the crack surfaces being governed by the opening displacement. The theoretical formulation is obtained using the dilute model of distributed cracks and the solution of a single dielectric crack problem. It is observed that the effective electroelastic property of cracked piezoelectric media is nonlinear and sensitive to loading conditions. Different modes of crack deformation are predicted and discussed. Attention is paid to the transition between electrically permeable and impermeable crack models.

Keywords: Effective properties; Piezoelectricity; Electromechanical coupling; Dielectric cracks; Electric boundary conditions

1. Introduction

Piezoelectric materials have been widely used in electromechanical devices, such as actuators, sensors and transducers due to their strong electromechanical coupling. The newly developed piezoceramic materials are generally brittle and susceptible to cracking during manufacturing and service processes. It is, therefore, essential to evaluate the electromechanical behaviour of this type of piezoelectric materials in the presence of microcracks.

The existence and development of microcracks in solid media exert important influences on various aspects of material properties. The investigation on effective material properties of microcracked media is of great importance and has drawn significant attention from the research and industrial communities. For traditional microcracked solids where boundary conditions along the crack surfaces are well defined, various micromechanics schemes have been established to estimate the effective moduli. The simplest one is

* Corresponding author. Fax: +1-780-492-2200.
E-mail address: xiaodong.wang@ualberta.ca (X.D. Wang).

0020-7683/$ - see front matter
doi:10.1016/S0020-7683(03)00285-3

the dilute or noninteracting model (Kachanov, 1992, 1993), in which the interaction among cracks is neglected. When accounting for the effects of the microcrack interaction, one may estimate the effective moduli by using self-consistent method (Hori and Nemat-Nasser, 1983; Budiansky and O'Connell, 1976), the differential method (Norris, 1985; Hashin, 1988; Zimmerman, 1991), the Mori–Tanaka method (Mori and Tanaka, 1973; Benveniste, 1986; Weng, 1990), and the generalized self-consistent method (Aboudi and Benveniste, 1987; Huang et al., 1994). In all these methods, it is assumed that the microcracked solids are statistically homogeneous and subjected to uniform tractions or displacements.

Relatively fewer studies have been conducted to deal with the effective electroelastic property of piezoelectric materials. The models mentioned above have been modified and used to study this type of materials. The effective electroelastic moduli of fiber reinforced piezoelectric composites were predicted by using the self-consistent method based on a concentric cylinder model (Grekov et al., 1989). Dunn and Taya (1993a,b) estimated the effective properties of piezoelectric composites using dilute, self-consistent, Mori–Tanaka and differential micromechanics models. The effective thermo-electro-elastic moduli of multiphase fibrous composites were studied by Chen (1994). Yu and Qin (1996) evaluated the thermo-electro-elastic properties of microcracked piezoelectric materials using the generalized self-consistent method.

It should be noted that for microcracked piezoelectric media, the electric boundary condition along crack surfaces is still one of the fundamental issues requiring further investigation, which may have important influence on the effective electroelastic property. Existing studies on the effective properties of cracked piezoelectric materials, as mentioned above, have been limited mostly to two typical crack models using different electric boundary conditions, i.e. electrically permeable model (Parton, 1976; Wang, 2001) and electrically impermeable model (e.g., Deeg, 1980; Pak, 1990; Suo et al., 1995; Park and Sun, 1995). These models represent two limiting cases where the electric permittivity of the crack is infinite and zero, respectively. Elliptical crack models (McMeeking, 1989; Sosa, 1991; Dunn, 1994; Zhang et al., 1998) has been used to study the effect of initial crack opening and the dielectric medium inside a crack upon electric boundary conditions. The results indicate that the permeable condition may underestimate the effect of the electric field on the crack propagation and impermeable model may overestimate its effect. For a slit crack, since the dielectric constant of piezoceramics is much higher than that of the air (or vacuum) filling the crack, the electric boundary condition may be very sensitive to the crack opening caused by the applied mechanical and electric loads (Wang, 2001; Wang and Jiang, 2002a,b). As a result, the electric boundary condition along the crack surfaces becomes deformation-dependent, which results in nonlinear response of the cracked medium to the applied loads and may significantly affect the effective electroelastic property.

It is therefore the objective of the current paper to provide a theoretical study of the effective electroelastic property of microcracked piezoelectric materials. A dielectric crack model with deformation-dependent electric boundary conditions in conjunction with a dilute model of interacting cracks are used to determine the nonlinear behaviour of the cracked medium. Special attention is paid to the effect of the dielectric medium filling the crack upon the effective electroelastic properties and the transition between permeable and impermeable crack models with increasing crack opening.

2. Statement of the problem

The plane problem envisaged in the current paper is to determine the effective electroelastic property of a piezoelectric medium weakened by parallel distributed cracks filled with a dielectric medium with negligible mechanical moduli. Assume that the microcracked piezoelectric medium can be modelled by a representative volume element (RVE) of volume Ω with unit thickness in z-direction and area A in xoy plane as shown in Fig. 1. The effective electroelastic property of this cracked medium can be derived by considering the relation between the volume averages of two piezoelectric field variables $\overline{\mathbf{\Phi}}$ and $\overline{\mathbf{Z}}$,

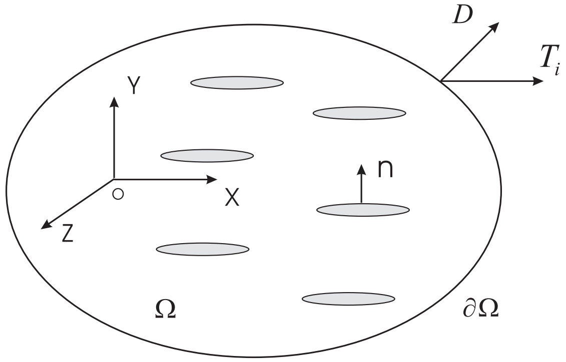

Fig. 1. The RVE model with parallel cracks.

$$\overline{\mathbf{\Phi}} = \frac{1}{\Omega}\int \mathbf{\Phi}\, d\Omega \tag{1}$$

$$\overline{\mathbf{Z}} = \frac{1}{\Omega}\int \mathbf{Z}\, \mathrm{d}\Omega \tag{2}$$

where $\mathbf{\Phi}$ and $\mathbf{Z}$ are defined as,

$$\mathbf{\Phi} = \{\Phi_{11}, \Phi_{22}, \Phi_{12}, \Phi_{31}, \Phi_{32}\}^{\mathrm{T}} \tag{3}$$

$$\mathbf{Z} = \{Z_{11}, Z_{22}, 2Z_{12}, Z_{31}, Z_{32}\}^{\mathrm{T}} \tag{4}$$

with the components of these vectors being given by

$$\Phi_{Ij} = \begin{cases} \sigma_{Ij} & I, j = 1, 2 \\ D_j & I = 3, \ \ j = 1, 2 \end{cases} \tag{5}$$

$$Z_{Ij} = \begin{cases} (u_{I,j} + u_{j,I})/2 & I, j = 1, 2 \\ V_{,j} & I = 3, \ \ j = 1, 2 \end{cases} \tag{6}$$

σ_{Ij}, u_I, D_j and V are the stress, the displacement, the electric displacement and electric potential, respectively. In the current paper, bold letter denotes matrix/vector quantities.

The general relation between $\overline{\mathbf{Z}}$ and $\overline{\mathbf{\Phi}}$ can be expressed as,

$$\overline{\mathbf{Z}} = \mathbf{S}\overline{\mathbf{\Phi}} \tag{7}$$

with $\mathbf{S}$ being the generalized compliance matrix of the effective medium, which may depend on $\overline{\mathbf{\Phi}}$. Suppose the boundary $\partial\Omega$ of the RVE is subjected to tractions T_i and electric displacement D, which correspond to a uniform stress and electric displacement field $\mathbf{\Phi}^0 = \{\sigma^0_{11}, \sigma^0_{22}, \sigma^0_{21}, D^0_1, D^0_2\}$ with $T_i = \sigma^0_{ij}\bar{n}_j$, $D = D^0_j\bar{n}_j$ and $\bar{n}_j$ being the components of outward normal of $\partial\Omega$. The averaged stress and electric displacement in the cracked medium can be obtained using Eq. (1) as,

$$\overline{\mathbf{\Phi}} = \mathbf{\Phi}^0 \tag{8}$$

Using the average scheme of Eq. (2), the average strain and electric field density $\overline{\mathbf{Z}}$ can be decomposed into two parts as discussed for traditional cracked media by Nemat-Nasser and Hori (1993),

$$\overline{\mathbf{Z}} = \mathbf{Z}^{\mathrm{m}} + \mathbf{Z}^{\mathrm{c}} \tag{9}$$

where $\mathbf{Z}^{m}$ can be determined by,

$$\mathbf{Z}^{m} = \mathbf{S}^{m}\mathbf{\Phi}^{0} \tag{10}$$

with $\mathbf{S}^{m}$ being the generalized compliance of the host medium. $\mathbf{Z}^{c}$ is caused by the presence of microcracks, the components of this vector can be determined by the displacement and electric potential jumps across crack surfaces (Nemat-Nasser and Hori, 1993; Yu and Qin, 1996). $\mathbf{Z}^{c}$ can be generally expressed as,

$$\mathbf{Z}^{c} = \mathbf{S}^{c}\mathbf{\Phi}^{0} \tag{11}$$

where $\mathbf{S}^{c}$ is a matrix to be determined through the crack surface deformation. Using Eqs. (7)–(11), the effective compliance of microcracked piezoelectric media becomes,

$$\mathbf{S} = \mathbf{S}^{m} + \mathbf{S}^{c} \tag{12}$$

3. Effective electroelastic properties of cracked piezoelectric media

There are two important issues in the determination of matrix $\mathbf{S}^{c}$ of cracked media through the use of different micromechanics models, the crack model and the interaction of cracks. In the current paper, 'real' electric boundary condition along crack surfaces will be considered using a dielectric crack model, and a dilute scheme will be used to treat crack interaction.

3.1. A dielectric crack

Consider a plane problem of a slit crack of length $2a$ filled with a dielectric medium with negligible mechanical moduli in an infinite piezoelectric medium with the poling direction along y, as shown in Fig. 2. Similar to the traditional crack model, the crack surfaces are traction free, i.e.,

$$\overline{\sigma}_{22}^{+} = \overline{\sigma}_{22}^{-} = 0 \tag{13}$$

When this slit crack is deformed, the thickness of the dielectric medium filling the crack will be changed, which will influence the overall dielectric property of the crack. As a result, the electric boundary condition along the crack surfaces will be deformation-dependent, unlike the existing crack models where only the original dimension of the crack is used (see, McMeeking, 1989; Dunn, 1994; Zhang et al., 1998).

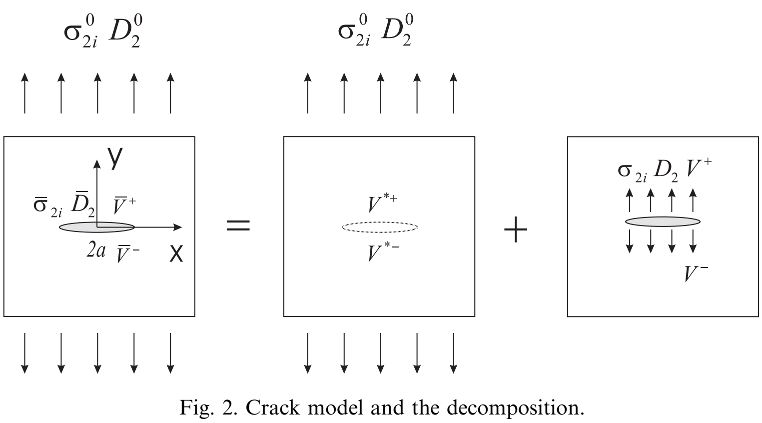

Fig. 2. Crack model and the decomposition.

For cases where opening deformation is significantly smaller than the crack length, it is assumed that the electric field intensity $\overline{E}_2$ and the electric displacement $\overline{D}_2$ are uniform across the thickness of the deformed crack, with

$$\overline{E}_2 = -\frac{1}{d_2}(\overline{V}^+ - \overline{V}^-) \tag{14}$$

$$\overline{D}_2 = \epsilon_0 \overline{E}_2 \quad \text{or} \quad \overline{D}_2 = -\epsilon_0 \frac{1}{d_2}(\overline{V}^+ - \overline{V}^-) \tag{15}$$

where $d_2 = u_2^+ - u_2^-$ is the opening displacement of the crack with superscripts + and − representing the upper and lower surfaces of the crack, respectively. ϵ_0 is the dielectric constant of the medium inside the crack.

The original crack problem (a) in Fig. 2 can be decomposed into the superposition of two subproblems (b) and (c). Subproblem (b) contains a uniform medium subjected to the applied mechanical and electric loading at infinity, and (c) includes a crack subjected to both mechanical and electric loads along its surfaces. The deformed geometry is used in (c) for the electric boundary condition. By using superposition principle on the deformed geometry, the traction free condition given by (13) can be expressed as,

$$\sigma_{2i}^+ = \sigma_{2i}^- = \sigma_{2i}, \quad \sigma_{2i} + \sigma_{2i}^0 = 0 \tag{16}$$

and the electric boundary condition (15) becomes

$$D_2^+ = D_2^- = D_2; \quad D_2 + D_2^0 = \epsilon_0(E_2 + E_2^*) \tag{17}$$

where $E_2 = -(V^+ - V^-)/d_2$, and $E_2^* = -(V^{*+} - V^{*-})/d_2$ is the applied electric field intensity.

For cases where the dielectric constant of the piezoelectric medium is much higher than ϵ_0, air filled crack for example, the additional term $\epsilon_0 E_2^*$ in (17) can be ignored in comparison with D_2^0. Eqs. (16) and (17) represent the deformation-dependent boundary condition of subproblem (c), which can be written in a matrix form as,

$$\mathbf{t} + \mathbf{t}^0 + \mathbf{K}(\mathbf{v}^+ - \mathbf{v}^-) = 0 \tag{18}$$

where $\mathbf{K}$ is a 3×3 matrix with only one nonvanishing element $k_{33} = \epsilon_0/d_2$. In addition, $\mathbf{t}^0 = \{\sigma_{21}^0, \sigma_{22}^0, D_2^0\}^{\mathrm{T}}$, $\mathbf{t} = \{\sigma_{21}, \sigma_{22}, D_2\}^{\mathrm{T}}$, and $\mathbf{v} = \{u_1, u_2, V\}$.

To solve this problem, the crack in subproblem (c) can be modelled in terms of the jumps of displacements and electric potential across the crack surfaces (Wang and Jiang, 2002a,b), as given in Appendices A and B,

$$\mathbf{t}(x, 0) = \int_{-a}^{a} \left(-\frac{1}{\pi(x - \xi)} \mathbf{H}^{-1} \right) \mathbf{d}'(\xi)\, \mathrm{d}\xi \tag{19}$$

where $\mathbf{d}' = \partial \mathbf{d}/\partial x$, $\mathbf{d}$ is the jumps of the displacement and electric potential across crack surfaces defined by,

$$\mathbf{d}(x) = \mathbf{v}^+(x, 0) - \mathbf{v}^-(x, 0) \tag{20}$$

and

$$\mathbf{H} = \begin{bmatrix} h_{11} & h_{12} & h_{13} \\ h_{22} & h_{22} & h_{23} \\ h_{31} & h_{32} & h_{33} \end{bmatrix} \tag{21}$$

is a constant matrix given in Appendix B. Making use of (19), the general boundary condition (18) becomes

$$\frac{1}{\pi}\int_{-a}^{a}\frac{\mathbf{\Gamma}'}{\xi-x}\,\mathrm{d}\xi+\mathbf{t}^0+\mathbf{KH\Gamma}=0 \tag{22}$$

where $\mathbf{\Gamma}=\mathbf{H}^{-1}\mathbf{d}$.

Singular integral equation (22) includes a square-root singularity and can be solved using Chebyshev polynomials,

$$\mathbf{\Gamma}'(x)=\mathbf{m}T_1\left(\frac{x}{a}\right)\Bigg/\sqrt{1-\frac{x^2}{a^2}} \tag{23}$$

where $\mathbf{m}^{\mathrm{T}}=\{m_1,m_2,m_3\}$ is a vector to be determined and $T_1(x/a)$ is the first order Chebyshev polynomial of the first kind. The jumps of the displacement and the electric potential across the crack surfaces are obtained as,

$$\mathbf{d}=\begin{Bmatrix}\Delta u_1\\ \Delta u_2\\ \Delta V\end{Bmatrix}=-\begin{Bmatrix}h_{11}m_1+h_{12}m_2+h_{13}m_3\\ h_{21}m_1+h_{22}m_2+h_{23}m_3\\ h_{31}m_1+h_{32}m_2+h_{33}m_3\end{Bmatrix}\sqrt{a^2-x^2} \tag{24}$$

Substituting (23) into (22) results in

$$\mathbf{m}-\mathbf{KHm}\sqrt{a^2-x^2}=-\mathbf{t}^0 \tag{25}$$

The only nonvanishing element of K is $k_{33}=\epsilon_0/d_2$ with $d_2=\Delta u_2$ being the crack opening displacement. Then Eq. (25) is reduced to the following algebraic equations

$$\begin{aligned} m_1&=-\sigma_{21}^0\\ m_2&=-\sigma_{22}^0\\ m_3&=-D_2^0-\epsilon_0\frac{h_{31}m_1+h_{32}m_2+h_{33}m_3}{h_{21}m_1+h_{22}m_2+h_{23}m_3}\end{aligned} \tag{26}$$

from which, m_1, m_2 and m_3 can be determined from the applied mechanical and electric loading.

3.2. Effective electroelastic properties

In the current paper, the crack interaction is simplified using a dilute model, i.e. a microcrack is assumed to be surrounded by a pristine matrix. The crack surface deformation can then be determined directly from the single crack solution given in the previous subsection. It is assumed that N_α is the number of cracks of length $2a_\alpha$ in the RVE with $\alpha=1,2,3,\ldots$ representing cracks of different lengths. The averaged strain and electric field intensity can then be expressed in terms of the jumps of the displacement and the electric potential across crack surfaces, similar to that obtained by Nemat-Nasser and Hori (1993) and Yu and Qin (1996) for traditional cracked materials and for piezoelectric materials with impermeable cracks,

$$Z_{Ij}^{\mathrm{c}}=\frac{1}{2A}\sum_{k=1}^{N}\int_{-a_k}^{a_k}\{[1+H(I-3)]d_In_j+H(2-j)d_jn_I\}\,\mathrm{d}s \tag{27}$$

where d_I are elements of the jumps of the displacement and the electric potential across crack surfaces given in Eq. (24), and n_k are elements of $\mathbf{n}=\{0,1,0\}^{\mathrm{T}}$.

Based on the result of d_I from the above mentioned dielectric crack model and making use of Eq. (24), the total contribution of cracks to the average strain and electric field intensity becomes,

$$Z_{Ij}^{\mathrm{c}}=\frac{\delta}{4}\{[1+H(I-3)]\Delta U_In_j+H(2-j)\Delta U_jn_I\} \tag{28}$$

where

$$\Delta U_I = -\sum_{k=1}^{3} h_{Ik} m_k \quad (I, k = 1, 2, 3) \tag{29}$$

are the jumps of the displacement and the electric potential at the centre of the crack, which contains the nonlinear effect of loading conditions represented by m_k, and δ is the crack density defined by,

$$\delta = \pi \sum_{\alpha=1}^{n} N_\alpha a_\alpha^2 / A$$

For a typical piezoceramic material with the poling direction along y, the generalized compliance matrix of the pristine medium $\mathbf{S}^{\mathrm{m}}$ is in the form of

$$\mathbf{S}^{\mathrm{m}} = \begin{bmatrix} f_{11} & f_{12} & 0 & 0 & p_{21} \\ f_{12} & f_{22} & 0 & 0 & p_{22} \\ 0 & 0 & f_{33} & p_{13} & 0 \\ 0 & 0 & p_{13} & k_{11} & 0 \\ p_{21} & p_{22} & 0 & 0 & k_{22} \end{bmatrix} = \begin{bmatrix} c_{11} & c_{12} & 0 & 0 & e_{12} \\ c_{21} & c_{22} & 0 & 0 & e_{22} \\ 0 & 0 & c_{33} & e_{31} & 0 \\ 0 & 0 & e_{31} & -\epsilon_{11} & 0 \\ e_{12} & e_{22} & 0 & 0 & -\epsilon_{22} \end{bmatrix}^{-1} \tag{30}$$

The material constants of PZT-4 piezoceramics (Park and Sun, 1995), for example, are

$$\begin{aligned} c_{11} &= 13.9 \times 10^{10}\ \mathrm{N/m^2} \\ c_{12} &= 7.43 \times 10^{10}\ \mathrm{N/m^2} \\ c_{22} &= 11.5 \times 10^{10}\ \mathrm{N/m^2} \\ c_{33} &= 2.56 \times 10^{10}\ \mathrm{N/m^2} \\ e_{12} &= -5.2\ \mathrm{C/m^2} \\ e_{22} &= 15.1\ \mathrm{C/m^2} \\ e_{31} &= 12.7\ \mathrm{C/m^2} \\ \epsilon_{11} &= 6.45 \times 10^{-9}\ \mathrm{C/Vm} \\ \epsilon_{22} &= 5.62 \times 10^{-9}\ \mathrm{C/Vm} \end{aligned}$$

For this type of materials, the generalized compliance of the cracked medium defined by (12) can be obtained from Eqs. (11), (28) and (30) as,

$$\mathbf{S} = \mathbf{S}^{\mathrm{m}} + \mathbf{S}^{\mathrm{c}} = \begin{bmatrix} s_{11} & s_{12} & 0 & 0 & s_{15} \\ s_{21} & s_{22} & 0 & 0 & s_{25} \\ 0 & 0 & s_{33} & s_{34} & 0 \\ 0 & 0 & s_{43} & s_{44} & 0 \\ s_{51} & s_{52} & 0 & 0 & s_{55} \end{bmatrix} \tag{31}$$

The elements of **S** are determined by the jumps of the displacement and electric potential across the crack surfaces, which are governed by the applied loads.

In the following discussion, attention will be paid to the determination of the elements of the compliance matrix **S** under different mechanical and electric loads. It should be mentioned that, because of the nonlinearity of the problem and the specific definition of **S** given by (12), the resulting **S** may not be symmetric.

3.2.1. Tensile loading

First, let the RVE under consideration be subjected to a stress field with $\sigma_{22}^0 \neq 0$ and $\sigma_{11}^0 = \sigma_{21}^0 = D_1^0 = D_2^0 = 0$. Eq. (26) results in $m_1 = 0$, $m_2 = -\sigma_{22}^0$ and two solutions for m_3, as

$$m_3^+ = \frac{1}{2h_{23}}(A - D); \quad m_3^- = \frac{1}{2h_{23}}(A + D) \tag{32}$$

where

$$A = h_{22}\sigma_{22}^0 - \epsilon_0 h_{33}; \quad B = 4h_{23}^2\epsilon_0\sigma_{22}^0; \quad D = \sqrt{A^2 + B}$$

m_3^+, m_3^- result in the opening and the overlapping of the crack surfaces, respectively, i.e. $\Delta u_2(m_3^+) > 0$, $\Delta u_2(m_3^-) < 0$. The solution corresponding to crack overlapping is not the one we are looking for since this phenomenon contradicts the original model of the crack. Therefore, for a tensile crack, only an open mode exists, for which the crack opening and the jump of electric potential ΔU_I at the centre of the crack can be determined using (29) as

$$\Delta U_2 = h_{22}\sigma_{22}^0 - h_{23}m_3^+ \tag{33}$$

$$\Delta U_3 = h_{32}\sigma_{22}^0 - h_{33}m_3^+ \tag{34}$$

Using these jumps along crack surfaces the corresponding effective elastic and piezoelectric parameters can be determined from Eq. (31) as,

$$s_{22} = f_{22} + \frac{\delta}{2}(h_{22}\sigma_{22}^0 - h_{23}m_3^+)/\sigma_{22}^0 \tag{35}$$

$$s_{52} = p_{22} + \frac{\delta}{2}(h_{32}\sigma_{22}^0 - h_{33}m_3^+)/\sigma_{22}^0 \tag{36}$$

$$s_{12} = f_{12} \tag{37}$$

3.2.2. Shear loading

For the case where only the shear stress σ_{21}^0 is applied, two solutions can be found $m_3 = 0$ and $m_3 = -\epsilon_0(h_{33}/h_{23})$. All these solutions correspond to closed crack. Since $h_{13} = 0$, the nonvanishing jumps of the displacement and electric potential ΔU_I can be expressed as,

$$\Delta U_1 = h_{11}\sigma_{21}^0 \tag{38}$$

$$\Delta U_3 = -h_{33}m_3 \tag{39}$$

Correspondingly, the following effective elastic and piezoelectric parameters can be derived,

$$s_{33} = f_{33} + \frac{\delta}{2}h_{11} \tag{40}$$

$$s_{43} = p_{13} \tag{41}$$

3.2.3. Electric loading

When electric displacement D_2^0 is applied and $\sigma_{11}^0 = \sigma_{22}^0 = \sigma_{21}^0 = D_1^0 = 0$. Two solutions of m_3 can be obtained as $m_3 = 0$ and $m_3 = -D_2^0 - \epsilon_0(h_{33}/h_{23})$. $m_3 = 0$ corresponds to a closed crack mode and has no effect upon the material properties. However, an opening crack mode represented by the second solution exists when the applied electric displacement satisfies $D_2^0 > -\epsilon_0(h_{33}/h_{23})$. The corresponding jumps of the displacement and electric potential ΔU_I are

$$\Delta U_2 = h_{23}\left(D_2^0 + \epsilon_0 \frac{h_{33}}{h_{23}}\right) \tag{42}$$

$$\Delta U_3 = h_{33}\left(D_2^0 + \epsilon_0 \frac{h_{33}}{h_{23}}\right) \tag{43}$$

The effective dielectric and piezoelectric parameters can be expressed as,

$$s_{55} = k_{22} + \frac{\delta}{2} h_{33}\left(D_2^0 + \epsilon_0 \frac{h_{33}}{h_{23}}\right) \Big/ D_2^0 \tag{44}$$

$$s_{25} = p_{22} + \frac{\delta}{2}(h_{23}D_2^0 + \epsilon_0 h_{33})/D_2^0 \tag{45}$$

$$s_{15} = p_{21} \tag{46}$$

3.2.4. Other loading conditions

When only mechanical loading σ_{11}^0 or electric displacement D_1^0 is applied, there will be no crack opening and the corresponding electroelastic parameters are same as that of the matrix, i.e.

$$s_{11} = f_{11} \tag{47}$$

$$s_{21} = f_{12} \tag{48}$$

$$s_{51} = p_{21} \tag{49}$$

$$s_{44} = k_{11} \tag{50}$$

$$s_{34} = p_{13} \tag{51}$$

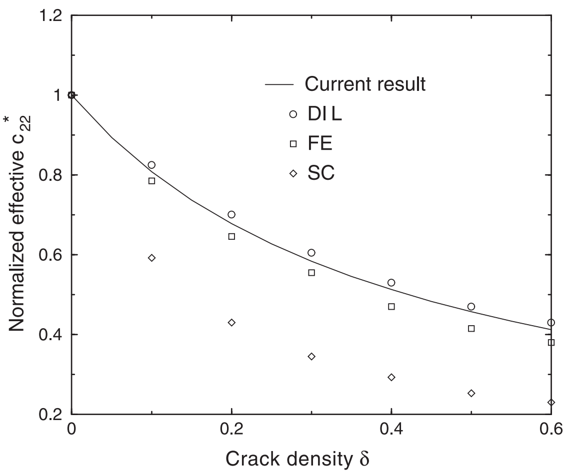

Fig. 3. Comparison for the normalized effective c_{22}^*.

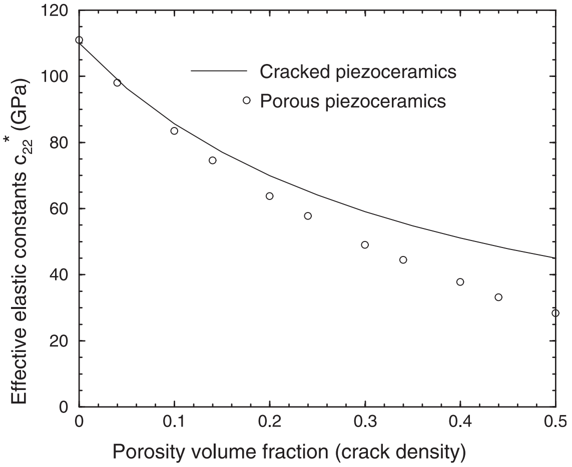

Fig. 4. Comparison between cracked and porous piezoceramics.

4. Results and discussion

First, we restrict our attention to the verification of the current solution. For isotropic elastic media weakened by parallel cracks, an analytical solution can be obtained, which predicts $c_{22}^* = 1/(1 + 2\delta)$. The result is supported by numerical calculations and is identical to that obtained by Kachanov (1992). To verify the current solution for piezoelectric media and evaluate the suitability of the dilute model (DIL) used, existing results of normalized stiffness $c_{22}^* = c_{22}/c_{22}^{\mathrm{m}}$ for $BaTiO_3$ weakened by parallel cracks (Qin et al., 1998) are compared in Fig. 3 with the result of the present solution based on the impermeable crack model. Excellent agreement is observed. Results from self-consistent (SC) method and finite element (FE) method are also included in Fig. 3. The comparison shows that, for the current problem, the dilute model provides reasonable prediction of the effective property of the cracked medium for the crack densities considered, as evidenced by the good agreement between the current result and that of the finite element method. Comparison is also made in Fig. 4 between the current solution, based on the impermeable crack

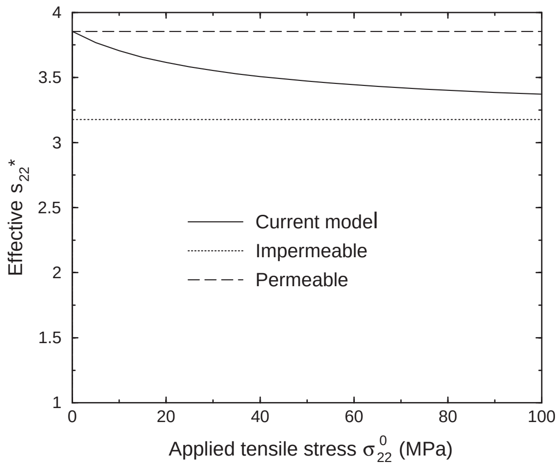

Fig. 5. The normalized effective s_{22}^* under tensile stress.

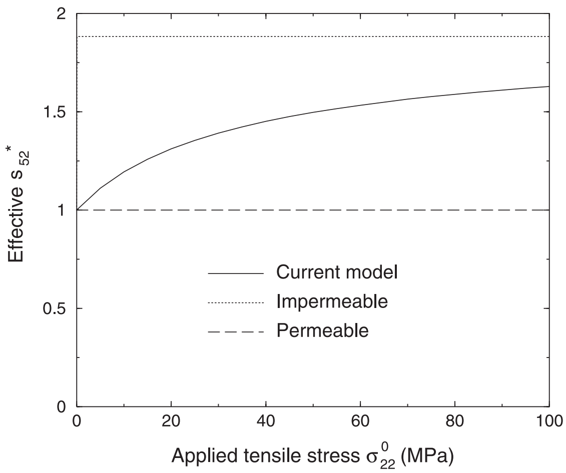

Fig. 6. The normalized effective s_{52}^* under tensile stress.

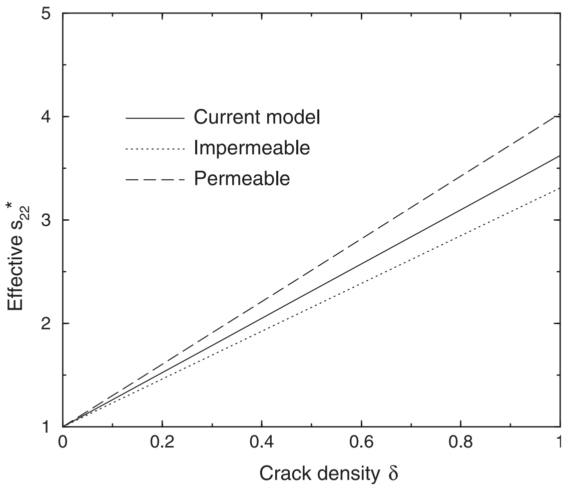

Fig. 7. Variations of s_{22}^* with crack density.

model, and that of a PZT-5$^+$ weakened by distributed spherical voids (Dunn and Taya, 1993b) with the crack density being assumed to be equal to the volume fraction of voids. A good agreement is observed for low crack densities.

The following discussion will be focussed on the numerical results of the effective electroelastic properties of cracked piezoelectric media, especially the transition between conventional impermeable and permeable models. Material constants of PZT-4 given in the previous section are used in the simulation. The dielectric medium filling the crack is assumed to be air with $\epsilon_0 = 8.85 \times 10^{-12}$ C/Vm.

The normalized effective parameter $s_{22}^* = s_{22}/f_{22}$ under tensile loading given by Eq. (35) is plotted in Fig. 5 with the crack density being $\delta = 0.3\pi$. It shows that this effective elastic modulus decreases with increasing tensile stress. But this effect is not significant. Corresponding results from impermeable and permeable crack models are also provided for comparison. The modulus from the current model is higher than the

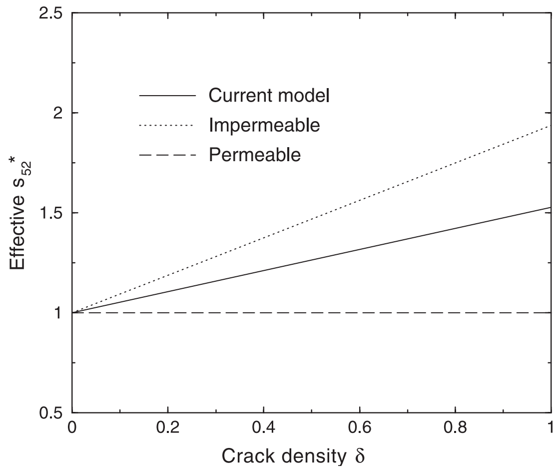

Fig. 8. Variations of s^*_{52} with crack density.

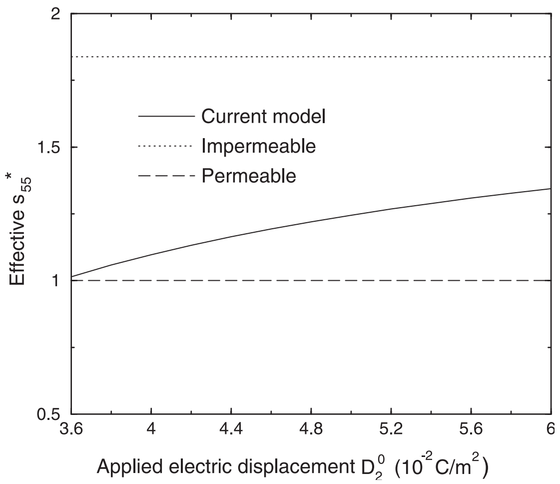

Fig. 9. The normalized s^*_{55} under electric loading.

result of the impermeable model but lower than that of the permeable one. For low stress, s^*_{22} is very close to the corresponding result using the permeable crack model. However, it approaches that of the impermeable model with increasing stress level. Fig. 6 shows the effect of applied tensile stress upon the normalized effective piezoelectric parameter $s^*_{52} = s_{52}/p_{22}$, which is greater than the permeable result but less than the impermeable one. Similar to s^*_{22}, it is observed from Fig. 6 that although the current result supports the permeable crack model when the stress level is low, with the increase of applied tensile stress the crack model will approach the impermeable one.

The effects of crack density upon the normalized effective parameters s^*_{22} and s^*_{52} are shown in Figs. 7 and 8, respectively for an applied tensile stress $\sigma^0_{22} = 50$ MPa. Both s^*_{22} and s^*_{52} are increasing with the increase of crack density for both current and impermeable crack models, although crack density δ shows no effect on the normalized effective piezoelectric parameter s^*_{52} from permeable model.

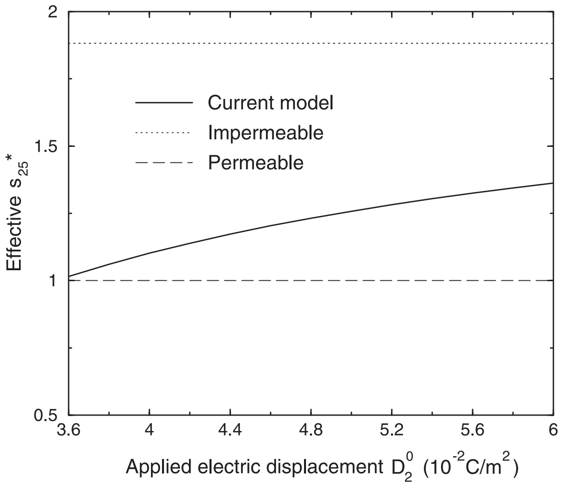

Fig. 10. The normalized s_{25}^* under electric loading.

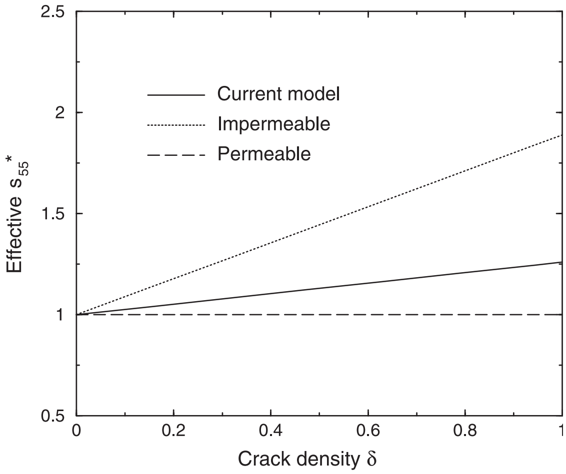

Fig. 11. Variations of s_{55}^* with crack density.

For shear loading, it is noted from Eq. (40) that crack density δ is the only parameter controlling s_{33}. s_{33} increases linearly with increasing crack density, which is identified to that by the impermeable and permeable models.

Fig. 9 shows the effect of an applied electric displacement D_2^0 upon the normalized dielectric parameter $s_{55}^* = s_{55}/k_{22}$ with the crack density $\delta = 0.3\pi$. s_{55}^* from the current model increases with increasing applied electric displacement and is always between the results from two conventional models. s_{55}^* approaches that of the permeable model when the applied electric displacement is low, as expected. Similar results for normalized piezoelectric parameter $s_{25}^* = s_{25}/p_{22}$ are plotted in Fig. 10. The effects of crack density upon the effective dielectric and piezoelectric parameters s_{55}^* and s_{25}^* under an applied $D_2^0 = 5.0 \times 10^{-2}$ C/m^2 are provided in Figs. 11 and 12, respectively.

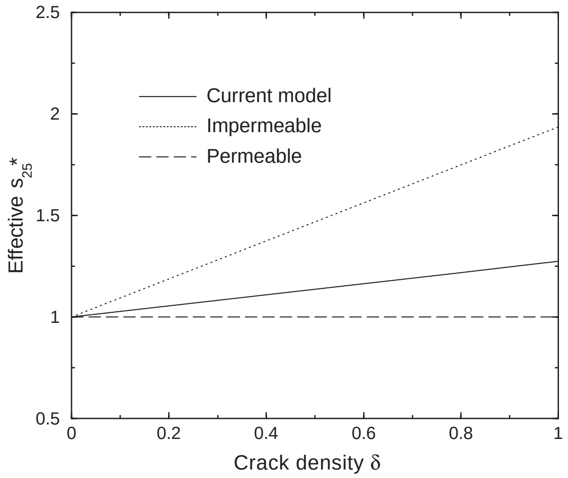

Fig. 12. Variations of s_{25}^* with crack density.

It should be noted that the effective s_{25}^* and s_{52}^* are load-dependent, which will cause the unsymmetry of the generalized effective compliance matrix. Significant discrepancy between the current model and the impermeable and permeable ones is observed, indicating that the dielectric property of the crack and the crack opening should be considered in determining the effective property of this type of materials.

5. Conclusions

A dielectric crack model is used to investigate the effective electroelastic property of piezoelectric media with parallel cracks. The jumps of the displacement and electric potential along crack surfaces are used for formulating the nonlinear electric boundary condition. Attention is focused on the parameters that control the effective electroelastic properties, the nonlinearity of these effective parameters and the transition between permeable and impermeable crack models under different loads. The current study indicates that the commonly used permeable and impermeable crack models represent two limiting cases which may not be suitable for predicting the effective property of cracked piezoelectric media.

Acknowledgement

This work was supported by the Natural Sciences and Engineering Research Council of Canada.

Appendix A

In the absence of free charges and body forces, the electromechanical behaviour of a piezoelectric medium is governed by the equilibrium equation and the Gauss' law,

$$\sigma_{ij,j} = 0; \quad D_{i,i} = 0 \tag{A.1}$$

and the constitutive equations,

$$\sigma_{ij} = c_{ijrs}\varepsilon_{rs} - e_{rij}E_r; \quad D_i = e_{irs}\varepsilon_{rs} + \epsilon_{ij}E_j \tag{A.2}$$

where c_{ijrs}, e_{irs} and ϵ_{ij} are elastic, piezoelectric and dielectric constants, respectively, $i, j, r, s = 1, 2, 3$, with 1, 2,3 corresponding to x, y and z, respectively. ε_{rs} and E_r are strain and electric field intensity defined by

$$\varepsilon_{rs} = \frac{1}{2}\left(\frac{\partial u_r}{\partial x_s} + \frac{\partial u_s}{\partial x_r}\right); \quad E_r = -\frac{\partial V}{\partial x_r} \tag{A.3}$$

with u_r and V being the displacement and the electric potential.

Consider a plane problem of a slit crack of length $2a$ in an infinite piezoelectric medium with poling direction along y, as shown in Fig. 2. A Cartesian coordinate system xoy is used to describe the crack plane. It is assumed that u_r and V depend only on in-plane coordinates, i.e. $u_r = u_r(x, y), r = 1, 2$ and $V = V(x, y)$. The system is subjected to a stress field $\sigma^0_{2i}(i = 1, 2)$ and electric displacement field D^0_2 at infinity. Correspondingly, Eq. (A.2) can be written in the matrix format as,

$$\begin{Bmatrix} \sigma_{11} \\ \sigma_{22} \\ \sigma_{12} \\ D_1 \\ D_2 \end{Bmatrix} = \begin{bmatrix} c_{11} & c_{12} & 0 & 0 & e_{12} \\ c_{21} & c_{22} & 0 & 0 & e_{22} \\ 0 & 0 & c_{33} & e_{31} & 0 \\ 0 & 0 & e_{31} & -\epsilon_{11} & 0 \\ e_{12} & e_{22} & 0 & 0 & -\epsilon_{22} \end{bmatrix} \begin{Bmatrix} \varepsilon_{11} \\ \varepsilon_{22} \\ 2\varepsilon_{12} \\ V_{,1} \\ V_{,2} \end{Bmatrix} \tag{A.4}$$

Substituting (A.2) and (A.3) into (A.1) results in the following governing equation of the problem,

$$(\mathbf{Q}X^2 + (\mathbf{R} + \mathbf{R}^{\mathrm{T}})XY + \mathbf{T}Y^2)\mathbf{v} = 0 \tag{A.5}$$

where $X = \partial/\partial x$, $Y = \partial/\partial y$, and

$$\mathbf{v}^{\mathrm{T}} = \{u_1, u_2, V\} \tag{A.6}$$

$$\mathbf{Q} = \begin{bmatrix} c_{11} & 0 & 0 \\ 0 & c_{33} & e_{31} \\ 0 & e_{31} & -\epsilon_{11} \end{bmatrix}$$

$$\mathbf{R} = \begin{bmatrix} 0 & c_{12} & e_{12} \\ c_{33} & 0 & 0 \\ e_{31} & 0 & 0 \end{bmatrix}$$

$$\mathbf{T} = \begin{bmatrix} c_{33} & 0 & 0 \\ 0 & c_{22} & e_{22} \\ 0 & e_{22} & -\epsilon_{22} \end{bmatrix}$$

Appendix B

A general dislocation can be defined by,

$$\mathbf{d}(x) = \mathbf{v}^+ - \mathbf{v}^- = \mathbf{d}_0 H(x), \quad y = 0 \tag{B.1}$$

with $\mathbf{v}^+$ and $\mathbf{v}^-$ representing the displacement and electric potential along upper and lower surfaces of the crack as defined in (A.6), $\mathbf{d}_0$ being a constant vector and $H(x)$ being the Heaviside step function.

Eq. (A.5) can be solved using Fourier transform with respect to x, which yields

$$-s^2\mathbf{Q}\mathbf{v}^* - \mathrm{i}s(\mathbf{R} + \mathbf{R}^{\mathrm{T}})\frac{\partial \mathbf{v}^*}{\partial y} + \mathbf{T}\frac{\partial^2 \mathbf{v}^*}{\partial y^2} = 0$$

with superscript '$*$' representing Fourier transform. The solution of $\mathbf{v}^*$ is generally in the form of

$$\mathbf{v}^* = \mathbf{a}\mathrm{e}^{-\mathrm{i}\eta y} \tag{B.2}$$

where **a** and η can be determined by solving the following eigenvalue problem

$$[\mathbf{Q} + p(\mathbf{R} + \mathbf{R}^{\mathrm{T}}) + p^2\mathbf{T}]\mathbf{a} = 0 \tag{B.3}$$

with $p = \eta/s$. It has been proved that this equation has no real roots (Suo et al., 1995). Let p_α be the eigenvalues with positive imaginary parts, $\mathbf{a}_\alpha$ the corresponding eigenvectors, and $\bar{p}_\alpha$ and $\bar{\mathbf{a}}_\alpha$ the conjugates of p_α and $\mathbf{a}_\alpha$, which are also the eigenvalues and eigenvectors of Eq. (B.3). To build a solution which vanishes at infinity, define $\eta_\alpha = p_\alpha s$, $\overline{\eta}_\alpha = \bar{p}_\alpha s$ for $s > 0$ and $\eta_\alpha = \bar{p}_\alpha s$, $\overline{\eta}_\alpha = p_\alpha s$ for $s < 0$. The general solution of $\mathbf{v}^*$ can then be expressed in terms of a linear combination of solutions given by (B.2) for different eigenvalues, such that

$$\mathbf{v}^* = (\mathbf{A}\mathbf{F}\mathbf{f}^r + \overline{\mathbf{A}}\mathbf{F}'\mathbf{g}^r)H(s) + (\overline{\mathbf{A}}\mathbf{F}\mathbf{f}^l + \mathbf{A}\mathbf{F}'\mathbf{g}^l)H(-s) \tag{B.4}$$

where $\mathbf{A} = [\mathbf{a}_1, \mathbf{a}_2, \mathbf{a}_3]$ and $\overline{\mathbf{A}} = [\bar{\mathbf{a}}_1, \bar{\mathbf{a}}_2, \bar{\mathbf{a}}_3]$ are known matrices determined by the eigenvectors. The matrices **F** and **F**′ are given by

$$\mathbf{F}(s, y) = \mathrm{diag}[\mathrm{e}^{-\mathrm{i}\eta_1 y}, \mathrm{e}^{-\mathrm{i}\eta_2 y}, \mathrm{e}^{-\mathrm{i}\eta_3 y}] \tag{B.5}$$

$$\mathbf{F}'(s, y) = \mathrm{diag}[\mathrm{e}^{-\mathrm{i}\overline{\eta}_1 y}, \mathrm{e}^{-\mathrm{i}\overline{\eta}_2 y}, \mathrm{e}^{-\mathrm{i}\overline{\eta}_3 y}] \tag{B.6}$$

f and **g** are coefficient vectors to be determined with the superscripts r and l representing the right $(s > 0)$ and left $(s < 0)$ half-planes. The corresponding stress and electric displacement fields can be expressed as,

$$\mathbf{t} = \mathbf{R}^{\mathrm{T}}\frac{\partial \mathbf{v}}{\partial x} + \mathbf{T}\frac{\partial \mathbf{v}}{\partial y} \tag{B.7}$$

with $\mathbf{t}^{\mathrm{T}} = \{\sigma_{21}, \sigma_{22}, D_2\}$.

From Eq. (B.4), the stress and electric displacement fields due to a dislocation defined by (B.1) can then be obtained using Fourier and inverse Fourier transforms, as

$$\mathbf{t} = -\frac{1}{\pi}\mathbf{H}^{-1}\mathbf{d_0}\frac{1}{x}, \quad y = 0 \tag{B.8}$$

where

$$\mathbf{H} = -2\mathrm{Im}(\mathbf{A}\mathbf{B}^{-1}) \tag{B.9}$$

H is symmetric and only the last element h_{33} is negative (Suo et al., 1995). Matrix **B** is defined by,

$$\mathbf{B} = \mathbf{R}^{\mathrm{T}}\mathbf{A} + \mathbf{T}\mathbf{A}\mathbf{P} \tag{B.10}$$

with **R** and **T** being given before and $\mathbf{P} = \mathrm{diag}[p_1, p_2, p_3]$.

References

Aboudi, J., Benveniste, Y., 1987. The effective moduli of cracked bodies in plane deformations. Engineering Fracture Mechanics 26, 171–184.

Benveniste, Y., 1986. On the Mori–Tanaka's method in cracked bodies. Mechanics Research Communication 13, 193–201.

Budiansky, Y., O'Connell, R.J., 1976. Elastic moduli of a cracked solid. International Journal of Solids and Structures 12, 81–92.

Chen, T., 1994. Micromechanical estimates of the overall thermoelectricelastic moduli of multiple fibrous composites. International Journal of Solids and Structures 31, 3099–3111.

Deeg, W.E.F., 1980. The analysis of dislocation, crack, and inclusion problems in piezoelectric solids. Ph.D. thesis, Stanford University.

Dunn, M.L., 1994. The effects of crack face boundary conditions on the fracture mechanics of piezoelectric solids. Engineering Fracture Mechanics 48, 25–39.
Dunn, M.L., Taya, M., 1993a. Micromechanics predictions of the effective electro-elastic moduli of piezoelectric composites. International Journal of Solids and Structures 30, 161–175.
Dunn, M.L., Taya, M., 1993b. Electromechanical properties of porous piezo-electric ceramics. Journal of American Ceramics Society 76 (7), 1697–1706.
Grekov, A.A., Kramarov, S.O., Kuprienko, A.A., 1989. Effective properties of a transversely isotropic piezocomposite with cylindrical inclusions. Ferroelectrics 99, 115–126.
Hashin, Z., 1988. The differential scheme and its application to cracked materials. Journal of Mechanics and Physics in Solids 36, 719–734.
Hori, H., Nemat-Nasser, S., 1983. Overall moduli of solids with microcracks: load-induced anisotropy. Journal of Mechanics and Physics in Solids 33, 155–171.
Huang, Y., Hu, K.X., Chandra, A., 1994. A generalized self-consistent mechanics method for microcracked solids. Journal of Mechanics and Physics in Solids 42, 1273–1291.
Kachanov, M., 1992. Effective elastic properties of cracked solids: critical review of some basic concepts. Applied Mechanics Review 45, 304–335.
McMeeking, R.M., 1989. Electrostrictive stresses near crack-like flaws. Journal of Applied Mathematics and Physics 40, 615–627.
Mori, T., Tanaka, K., 1973. Average stress in matrix and average elastic energy of materials with misfitting inclusions. Acta Metallurgica 21, 571–574.
Nemat-Nasser, S., Hori, M., 1993. Micromechanics: Overall Properties of Heterogeneous Materials. North-Holland, Amsterdam, New York.
Norris, A.N., 1985. A differential scheme the effective moduli of composites. Mechanics of Materials 4, 1–16.
Pak, Y.E., 1990. Crack extension force in a piezoelectrical material. Journal of Applied Mechanics 57, 647–653.
Park, S., Sun, C.T., 1995. Fracture criteria for piezoelectric ceramics. Journal of American Ceramic Society 78, 1475–1480.
Parton, V.Z., 1976. Fracture mechanics of piezoelectric materials. Acta Astronaut 3, 671–683.
Qin, Q., Mai, Y., Yu, S., 1998. Effective moduli for thermopiezoelectric materials with microcracks. International Journal of Fracture 91, 359–371.
Sosa, H., 1991. Plane problems in piezoelectric media with defects. International Journal of Solids and Structures 28, 491–505.
Suo, Z., Kuo, C.M., Barnett, D.M., Willis, J.R., 1995. Fracture mechanics for piezoelectric ceramics. Journal of Mechanics and Physics of Solids 40, 739–765.
Wang, X.D., 2001. On the dynamic behavior of interacting interfacial cracks in piezoelectric media. International Journal of Solids and Structures 38, 815–831.
Wang, X.D., Jiang, L.Y., 2002a. Fracture behaviour of cracks in piezoelectric media with electromechanically coupled boundary conditions. Proceedings of the Royal Society of London, Series A 458, 2545–2560.
Wang, X.D., Jiang, L.Y., 2002b. Nonlinear behaviour of interacting dielectric cracks in piezoelectric materials. International Journal of Solids and Structures 39, 585–600.
Weng, G., 1990. The theoretical connection between Mori–Tanaka's theory and the Hashin–Shtrikman–Walpole bounds. International Journal of Engineering Science 28, 1111–1120.
Yu, S.W., Qin, Q.H., 1996. Damage analysis of thermopiezoelectric properties: Part II. Effective crack model. Theoretical and Applied Fracture Mechanics 25, 279–288.
Zhang, T.Y., Qian, C.F., Tong, P., 1998. Linear electro-elastic analysis of a cavity or a crack in a piezoelectric material. International Journal of Solids and Structures 35 (17), 2121–2149.
Zimmerman, R.W., 1991. Elastic moduli of a solid containing spherical inclusions. Mechanics of Materials 12, 17–24.